Electronic structure of $TlBa_2CaCu_2O_{7-\delta}$

R. P. Vasquez
Center for Space Microelectronics Technology, Jet Propulsion Laboratory, California Institute of Technology, Pasadena, California 91109-8099

D. L. Novikov and A. J. Freeman
Science and Technology Center for Superconductivity, Department of Physics and Astronomy, Northwestern University, Evanston, Illinois 60208-3112

M. P. Siegal
Sandia National Laboratories, Albuquerque, New Mexico 87185-1421

(Received 25 November 1996)

The core levels of $TlBa_2CaCu_2O_{7-\delta}$ (Tl-1212) epitaxial films have been measured with x-ray photoelectron spectroscopy (XPS). The valence electronic structure has been determined using the full-potential linear muffin-tin-orbital band-structure method and measured with XPS. The calculations show that a van Hove singularity (VHS) lies above the Fermi level (E_F) for the stoichiometric compound ($\delta=0$), while for 50% oxygen vacancies in the Tl-O layer ($\delta=0.5$) E_F is in close proximity to the VHS. Samples annealed in nitrogen (to reduce the hole overdoping by the removal of oxygen) exhibit higher core-level binding energies and a higher T_c, consistent with a shift of E_F closer to the VHS. Comparisons are made to the core levels and valence bands of $Tl_2Ba_2CaCu_2O_{8+\delta}$ (Tl-2212) and $HgBa_2CaCu_2O_{6+\delta}$ (Hg-1212). The similarity of the Cu $2p_{3/2}$ spectra for Tl-1212 and Tl-2212 indicates that the number of Tl-O layers has little effect on the Cu-O bonding. However, the Tl-1212 and Hg-1212 Cu $2p_{3/2}$ signals exhibit differences which suggest that the replacement of Tl^{3+} with Hg^{2+} results in a decrease in the O $2p\rightarrow$Cu $3d$ charge-transfer energy and differences in the probabilities of planar vs apical oxygen charge transfer and/or Zhang-Rice singlet-state formation. Differences between the Tl-1212 and the Tl-2212 and Hg-1212 measured valence bands are consistent with the calculated Cu $3d$ and (Tl,Hg) $6s/5d$ partial densities of states. [S0163-1829(97)04721-8]

I. INTRODUCTION

Among the Tl-cuprate high-temperature superconductors, the $TlBa_2Ca_{n-1}Cu_nO_{3+2n-\delta}$ [Tl-12$(n-1)n$] family has received little attention relative to the Tl-22$(n-1)n$ family, due to both the somewhat lower superconducting transition temperatures (T_c) and the greater difficulty in obtaining high-quality Tl-12$(n-1)n$ phases. Comparison of single- and double-Tl-layer materials is of fundamental interest in determining the effect of the charge reservoirs and distance between Cu-O planes on the electronic structure. However, band-structure calculations of single-Tl-layer materials have been limited to a single tight-binding study.[1]

Some interest in applications of the Tl-1223 phase has been motivated by its lower anisotropy, greater flux pinning, and consequently higher critical current densities relative to the more commonly studied Tl-2212 and Tl-2223 phases. The Tl-1212 phase also has greater flux pinning, but has been the subject of even fewer studies. The T_c of Tl-1212 depends sensitively on the oxygen doping,[2] varying in bulk powders from 80 K for samples synthesized in oxygen to as high as 110 K as δ increases, thus requiring controlled annealing in an inert atmosphere to achieve optimal doping by removal of excess oxygen. The growth of high-quality epitaxial Tl-1212 films, which are of interest for microwave device applications, has only recently been demonstrated.[3,4]

High-temperature superconductors have been widely studied with photoemission spectroscopy. Valence-band measurements provide a measure of the density of states, while core-level measurements provide information on issues such as oxidation states and doping-induced chemical potential shifts and, in the case of the highly correlated Cu cations, charge-transfer mechanisms and multiplet splitting. However, photoemission studies of the Tl cuprates have been limited by the difficulty in obtaining well-characterized, high-quality materials, as well as by the well-known difficulty, common to all of the cuprates, in obtaining clean surfaces due to the reactivity of the alkaline-earth components. Previous x-ray photoelectron spectroscopy (XPS) measurements on Tl-1212 are limited to reports from a single group.[5–7] The earlier XPS studies reported no detectable Fermi edge and were on polycrystalline samples scraped in vacuum,[5–7] which can yield surfaces with significant spectral contributions from nonsuperconducting grain-boundary species and/or artifacts from scrape-induced damage.[8] XPS measurements from higher-quality Tl-1212 surfaces are therefore desirable.

In this work, XPS core-level and valence-band measurements are reported for high-quality epitaxial Tl-1212 films. These results are compared to the band structure calculated in this work and to previously reported XPS measurements of Tl-1212 polycrystalline pellets.[5–7] The Tl-1212 film surfaces are demonstrated to be high quality, as shown by the relatively low intensities observed for the high-binding-energy contaminant signals in the O $1s$ and Ba core levels and the observation of a clear Fermi edge in the valence-

band region. Comparison of the data measured in this work to earlier measurements on epitaxial films of Hg-1212 (Ref. 9) and Tl-2212 (Ref. 10) yields information on the effects of varying the number of Tl-O layers or replacing the Tl^{3+} with Hg^{2+}. The effects of oxygen doping are investigated by comparing XPS spectra from as-grown and nitrogen-annealed Tl-1212 samples with significantly different T_c's. The doping-induced core-level shifts and change in T_c are compared to expectations based on band-structure calculations, and the possible role of van Hove singularities is discussed. The measured Tl-1212 valence-band density of states is compared to those of Tl-2212 and Hg-1212, and differences are explained by comparison of the calculated Cu $3d$ and (Tl,Hg) $6s/5d$ partial densities of states of these materials.

II. EXPERIMENT

Epitaxial Tl-1212 films on $LaAlO_3$ (100) substrates are obtained by sputter deposition of Tl-free precursor films followed by an *ex situ* anneal in a static two-zone furnace for thallination. Details of the film growth, annealing, and characterization are described elsewhere.[4] Some of the films received an additional anneal in nitrogen at 250 °C for 1 h. Prior to the final nitrogen anneal, which adjusts the oxygen content, the films are typically superconducting at ~70–75 K, while T_c is raised to ~85–90 K after nitrogen annealing.

The films were cleaned with a nonaqueous etchant consisting of 0.1% Br_2 in absolute ethanol, rinsed in ethanol, and blown dry with nitrogen in the ultrahigh-purity nitrogen atmosphere of a glove box which encloses the XPS load lock. This procedure minimizes exposure of the clean surface to reactive atmospheric gases such as water vapor and carbon dioxide and has yielded high-quality surfaces for other cuprate superconductors,[8] notably including the Tl-cuprate phases Tl-2212 (Ref. 10) and Tl-2201 (Ref. 11) as well as the chemically and structurally similar Hg cuprate Hg-1212 (Ref. 9). The etch rate was found to be ~1000 Å/min, and a 45-s etch was sufficient for obtaining XPS spectra characteristic of high-quality surfaces, using criteria described elsewhere.[8] The XPS spectra were accumulated on a Surface Science Spectra SSX-501 spectrometer with monochromatized Al K_α^n x rays (1486.6 eV), photoemission normal to the film surface, and a base pressure of 5×10^{-10} Torr. The x-ray beam diameter was 150 μm for the core-level measurements and 300 μm for the valence-band measurements. The pass energy of the electron energy analyzer was 25 eV, yielding a peak full width at half maximum (FWHM) of 0.7 eV for a Au $4f_{7/2}$ signal. The Fermi level of Au is taken to be the zero of binding energy, which yields a Au $4f_{7/2}$ binding energy, measured from a deposited Au film, of 83.9 eV and a Cu $2p_{3/2}$ binding energy, measured from an Ar-ion-etched Cu plate, of 932.5 eV.

One fully oxygenated and two nitrogen-annealed films are measured in this work, and ac susceptibility measurements following the XPS measurements show a superconducting transition onset at 74.5 K with a transition width of 2 K for the oxygenated film, and superconducting transition onsets of 86 and 87 K with transition widths of 1 K for the nitrogen-annealed films. Equivalent XPS spectra are obtained from both nitrogen-annealed films; the spectra presented here are from the film with $T_c=87$ K. The surface stoichiometries after etching for all three films measured in this work are near Tl:Ba:Ca:Cu=1:1.85:1.15:2.

III. BAND-STRUCTURE CALCULATIONS

Since the oxygen content in Tl-O layers is of crucial importance for T_c, the electronic structure is calculated for Tl-1212 with two different oxygen contents; one corresponds to $\delta=0$ when all oxygen sites in the Tl-O layer are occupied, and another corresponds to $\delta=0.5$ when every other oxygen site is vacant.

To determine the electronic structure of Tl-1212, the full-potential linear muffin-tin orbital[12] (FLMTO) was used within the local density approximation (LDA) and the Ceperly-Alder form of the exchange-correlation potential. In these calculations no shape approximations are made to either the charge density or potential. The structural parameters for Tl-1212 are taken from Ref. 13. The unit cell consists of two Cu-O_2 layers [oxygen atoms in Cu-O_2 layers are referred to as O(1)] separated by Ca and a blocking layer containing Ba, ''apical'' oxygen [O(2)], and the Tl-O layer with its oxygen site referred to as O(3). Local atomic distortions around the oxygen vacancy site that were measured in Ref. 13 were taken into account in the calculations for Tl-1212 ($\delta=0.5$).

The FLMTO calculations are performed in the spin-restricted scalar-relativistic mode with atomic Ba($5s^25p^66s^26p^0$), Tl($5s^25p^65d^{10}6s^26p^1$), Cu($3s^23p^63d^{10}4s^1$), Ca($3s^23p^24s^2$), and O($2s^22p^4$) levels treated as valence-band electrons. A technique,[14] similar to Singh's ''local orbitals,''[15] is used to enable simultaneous treatment of orbitals with equal orbital number in the same energy window. It is well known that the LMTO scheme of band calculations works well for close-packed structures. In order to get a more close-packed structure, empty spheres are introduced at sites (0.5,0.0,0.0). The MT radii are carefully chosen based on the spatial distribution of the self-consistent charge density over the unit cell.

The set of radii $R_{Tl}=2.0$, $R_{Ba}=3.4$, $R_{Ca}=2.84$, and $R_O=1.8$ a.u. is used since these radii attribute charge densities centered at different atoms to their corresponding spheres, leaving only relatively smooth variations of the charge density over the interstitial region. A triple-κ basis set is employed for each type of atom with angular momentum l up to 2 for Tl, Cu, and O and up to 3 for Ba and Ca for $\kappa^2=-0.01$ Ry, and up to 1 for $\kappa^2=-1.0$ and -2.3 Ry. Wave functions with $l_{max}=1$ are associated with empty spheres for the first κ value only. The charge density is calculated exactly in muffin-tin spheres for angular momentum components up to $l=6$. The same l cutoff is used when interpolating in the interstitial region over Hankel functions with energies -1 and -3 Ry. Calculations done for $l=5$ do not show any difference in band positions, which indicates good convergence of the results with l_{max}.

The Brillouin-zone (BZ) integrations are carried out by the tetrahedron method using a 455-k-point mesh (corresponding to $12\times12\times12$ regular divisions along the k_x, k_y, and k_z axes, respectively) in the 1/16 irreducible wedge.

The total and l-projected densities of states (DOS) of Tl-1212 ($\delta=0$) are presented in Fig. 1 with the Fermi energy

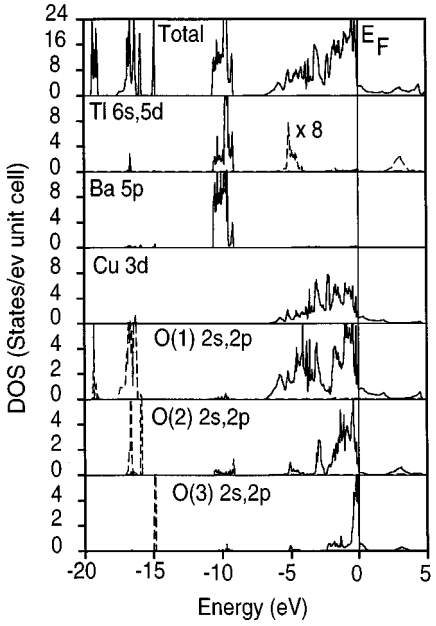

FIG. 1. Total and l-projected DOS for Tl-1212 ($\delta=0$). The Tl $6s$ and O $2s$ DOS are shown by dashed lines. The scale for the Tl $6s$ states is enlarged by a factor of 8.

(E_F) chosen at 0 eV. The upper part of the valence band consists of strongly hybridized Cu $3d$ and O(1,2,3) $2p$ states. The effective width of the O $2p$ states decreases from O(1) to O(2) and O(3), reflecting a reduction of the covalent bonding of oxygen in different crystallographic positions. The part of the valence band located around -10 eV consists mostly of Tl $5d$ and Ba $5p$ states with Tl $5d$ states lying slightly above the Ba $5p$. The states at -16 eV are composed mainly of O $2s$ states. A clear shift of the O $2s$ states for O(1), O(2), and O(3) suggests different degrees of ionization, being the least for oxygen in Tl-O layers. Another interesting feature is that O(3) has a very narrow $2p$ band [compared to O(1) and O(2)], which suggests that O(3) is incorporated in the structure as a loosely bonded ion. Thus annealing in an inert atmosphere most probably affects only oxygen in Tl-O layers.

The band structure in the range from -18 to $+5$ eV relative to E_F presented in Fig. 2 also shows three distinct groups of bands: In the upper energy are Cu-O-hybridized bands, Ba $5p$–Tl $5d$ in the middle and O $2s$ states at the bottom with a very flat band of O(3) $2s$ states.

Figure 3 presents the band structure in the vicinity of E_F which looks very similar to the band structures of all layered Cu-O-based high-T_c superconductors. Two almost-free-electron-like $dp\sigma$ bands (their number corresponds to the number of Cu-O layers) cross the Fermi level. One can see a prominent van Hove singularity (VHS) which is located along the X-R direction in the BZ, as is usual for all tetragonal cuprate high-T_c materials.[16]

The total and l-decomposed DOS for Tl-1212 ($\delta=0.5$) are presented in Fig. 4. The introduction of oxygen vacancies in the Tl-O layer produces quite dramatic changes in the band structure of Tl-1212 (as compared to the $\delta=0$ case). First of all, the interaction strength of O(3) with the rest of the crystal is changed: The O(3) $2p$ bandwidth is enlarged

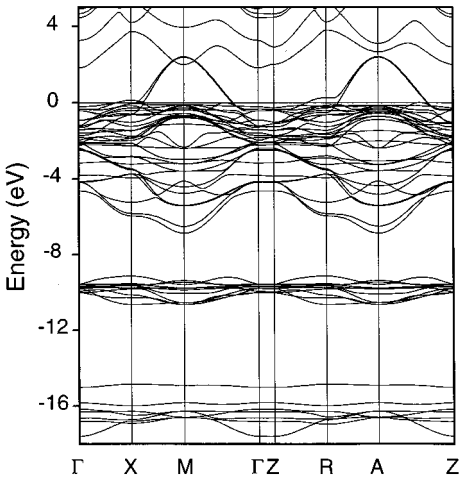

FIG. 2. FLMTO band structure along high-symmetry directions for Tl-1212 ($\delta=0$).

and shifts deeper below E_F (cf. Fig. 4), or alternatively E_F shifts up in energy; the O(3) $2s$ states are now located in nearly the same energy region as the O(1) $2s$ states, while the O(2) $2s$ states are shifted to approximately 2 eV below (higher binding energy than) the O(1) and O(3) $2s$ states. This changes the O $2s$ state ordering found for the Tl-1212 ($\delta=0$) case. Also, note that the Ba $5p$ states corresponding to the Ba atom with completely occupied O(3) sites are ~ 2 eV lower in energy (higher binding energy) than the $5p$ states of Ba with an O(3) vacancy in its nearest vicinity. Such changes in oxygen and Ba states are caused by strong changes in the Madelung potential of the Tl-O layers induced by partial removal of the O(3) atoms.

Another interesting feature of the Tl-1212 ($\delta=0.5$) electronic structure is the E_F location, which lies well below the VHS in Tl-1212 ($\delta=0$), but in Tl-1212 ($\delta=0.5$) is in close proximity to the VHS. This is clearly seen in Fig. 4, where E_F is close to the DOS maximum produced by the VHS.

IV. XPS CORE-LEVEL MEASUREMENTS

The core-level binding energies and peak FWHM measured in this work from as-grown and nitrogen-annealed Tl-

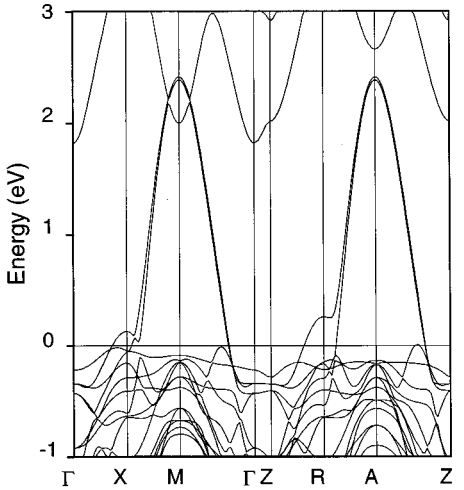

FIG. 3. FLMTO band structure in the Fermi-energy region for Tl-1212 ($\delta=0$).

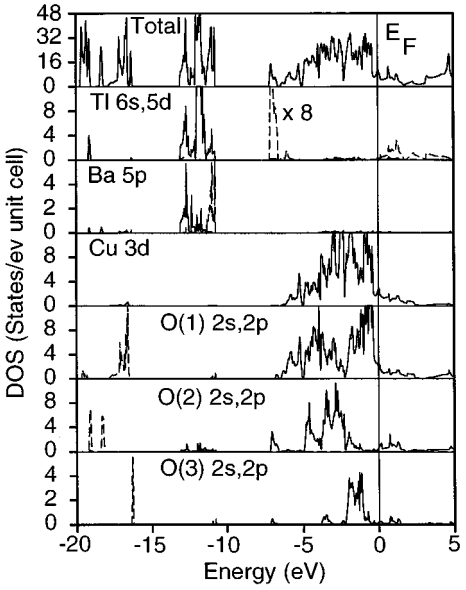

FIG. 4. Total and l-projected DOS for Tl-1212 ($\delta=0.5$). The Tl 6s, Ba [near the O(3) vacancy] 5p, and O 2s DOS are shown by dashed lines. The Tl 6s states are shown enlarged by a factor of 8.

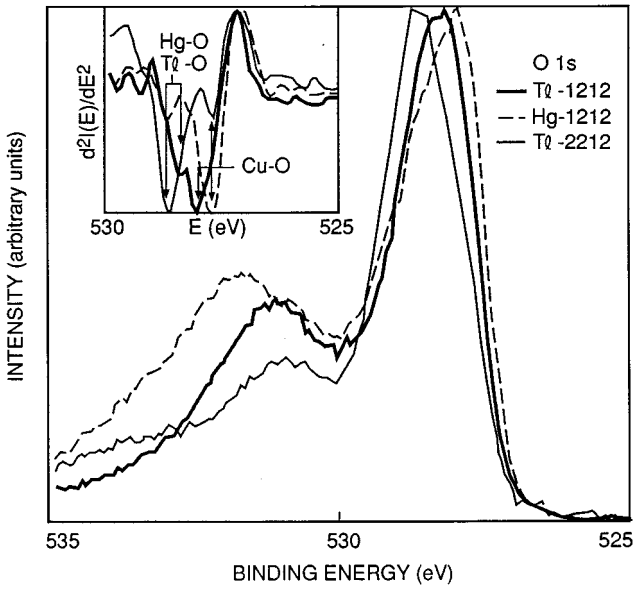

FIG. 5. O 1s spectra measured from chemically etched epitaxial films of Tl-1212 (this work), Tl-2212 (Ref. 10), and Hg-1212 (Ref. 9). The inset shows the second derivatives of the spectra.

1212 epitaxial films are summarized in Table I, together with measurements previously reported for Tl-1212 polycrystalline pellets[5–7] and for Hg-1212 and Tl-2212 epitaxial films.[9,10] The O 1s spectrum measured from a nitrogen-annealed Tl-1212 film after etching is compared in Fig. 5 to the corresponding spectra from Hg-1212 and Tl-2212 epitaxial films.[9,10] The peak near 531 eV, which is dominant prior to etching, is associated with contaminants,[8] particularly alkaline-earth carbonates. The lower-binding-energy manifold is a minor component prior to etching and originates from the nonequivalent oxygen sites in the Tl-1212 lattice. The dominance of the lower-binding-energy superconductor signals in Fig. 5 demonstrates the surface cleanliness obtained in this work. In contrast, earlier studies of polycrystalline Tl cuprates[5–7] exhibited O 1s spectra with contaminant and superconductor signals nearly equal in intensity.[6]

The Tl-1212 O 1s signal consists of two components, as demonstrated more clearly in the second derivatives of the spectra shown in the inset of Fig. 5. As previously mentioned, O(3) in the Tl-O planes is the oxygen with the lowest binding energy for $\delta=0$ and has nearly the same binding energy as the O(1) states for $\delta=0.5$. Assuming 75% O(3) occupancy for optimally doped Tl-1212,[13] the O(3) signal would account for only 11% of the total O 1s intensity and would be $<20\%$ of the intensity of the O(1) signal from Cu-O planes. The lowest-binding-energy signal which is re-

TABLE I. Summary of core-level binding energies (±0.05 eV), peak full widths at half maximum (in parentheses), and Cu $2p_{3/2}$ satellite to main peak (I_s/I_m) intensity ratios (±0.02) for Tl-1212 epitaxial films measured in this work, together with previously reported results for Tl-1212 polycrystalline pellets and for Tl-2212 and Hg-1212 epitaxial films.

Material	Tl $4f_{7/2}$	Ba $3d_{5/2}$	Ba $4d_{5/2}$	Ca $2p_{3/2}$	Cu $2p_{3/2}$	I_s/I_m	O 1s	Ref.
Tl-1212 ($T_c=87$ K)	117.75 (1.4)	778.09 (1.4)	87.67 (1.15)	344.61(1.2), 345.68(1.2)	933.1 (3.2)	0.44	527.99(1.0), 528.64(1.2)	this work
($T_c=86$ K)	117.83 (1.4)	778.13 (1.5)	87.71 (1.15)	344.61(1.3), 345.70(1.4)	933.1 (3.3)	0.42	528.02(1.0), 528.72(1.1)	this work
($T_c=74.5$ K)	117.66 (1.4)	777.99 (1.5)	87.56 (1.2)	344.57(1.2), 345.60(1.2)	933.1 (3.2)	0.43	527.93(1.0), 528.60(0.9)	this work
($T_c=73$–79 K)	117.7 (1.5)	778.8	not reported	345.0	933.3 (3.4)	0.41	~529	5–7
Tl-2212 ($T_c=102$ K)	118.02 (1.25)	778.27 (1.55)	87.87 (1.15)	344.66(1.2), 345.73(1.2)	933.1 (3.1)	0.45	527.84(0.9), 528.69(1.4)	10
Hg-1212 ($T_c=117$ K)	none	778.21 (1.45)	87.83 (1.1)	344.48(1.1), 345.62(1.2)	932.9 (3.4)	0.36	527.87(0.9), 528.72(1.1)	9

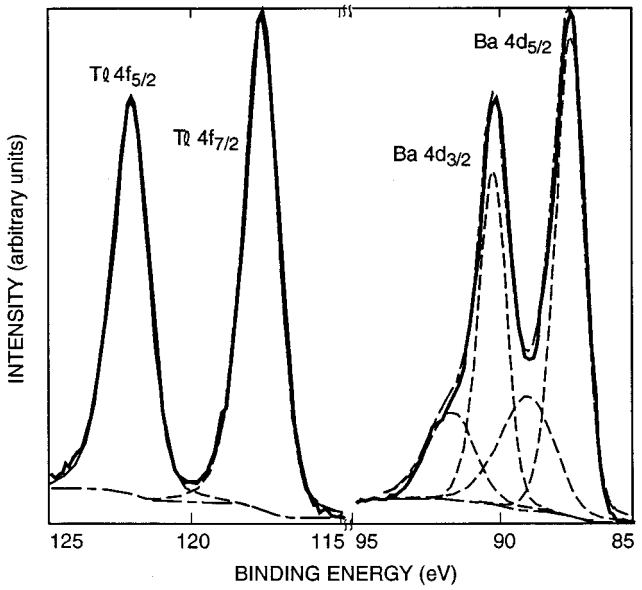

FIG. 6. Tl $4f$ and Ba $4d$ spectra measured for Tl-1212, together with the results of least-squares fitting.

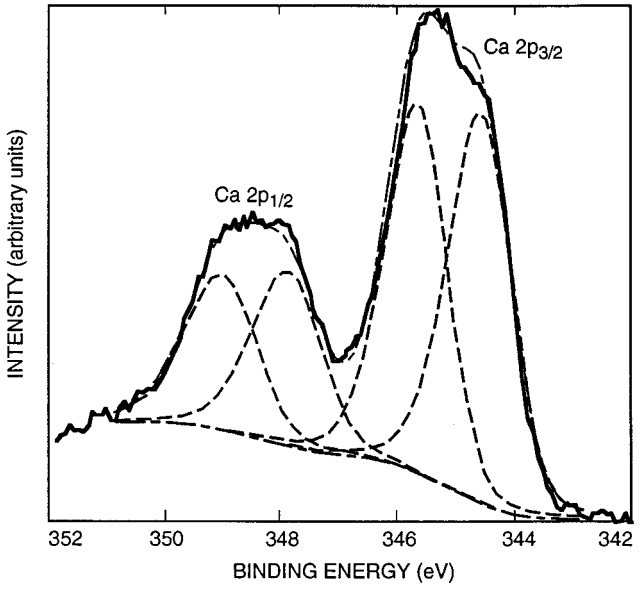

FIG. 7. Ca $2p$ spectrum measured for Tl-1212, together with the results of least-squares fitting.

solvable in Fig. 5 is the signal with the greatest intensity and is therefore assigned to Cu-O planes, consistent with studies of other cuprate superconductors.[9–11,17–21] The higher-binding-energy component is assigned to Tl-O(2) bonding, consistent with the O state ordering found in the band-structure calculations in this work and with previous experimental assignments.[10,11,19,21] The O(3) signal would either contribute to the O(1) signal or would be an unresolvably small component on the low-binding-energy side of the much more intense O(1) signal. These assignments are verified with angle-resolved measurements, which show that at a photoelectron emission angle 70° from normal the Tl, Ba, and higher-binding-energy O $1s$ core-level signals are enhanced relative to the Cu and lower-binding-energy O $1s$ core-level signals. These observations suggest Tl-O surface termination, consistent with previously reported measurements of chemically etched Tl-2212.[21] The relative Ca abundance is not angle dependent, which likely results from Ca occupying multiple lattice sites, as discussed later.

The O $1s$ signals of Tl-2212 and Hg-1212 also consist of two components, as shown for comparison in the inset of Fig. 5, with the high-binding-energy component of Hg-1212 being associated with Hg-O bonding. The two O $1s$ components have the same binding energies for Hg-1212 and Tl-2212, with different intensity ratios yielding the observed difference in the manifold line shapes. For Tl-1212 and Hg-1212, on the other hand, the difference in observed manifold line shapes originates from two O $1s$ components having similar intensities, but differing binding energies, with the energy separation being 0.3–0.4 eV less for Tl-1212.

The Tl $4f$ and Ba $4d$ spectra are presented in Fig. 6. A least-squares fitting shows that the Tl $4f$ spectrum is consistent with a single doublet, in agreement with previous measurements from Tl-1212 polycrystalline pellets scraped in vacuum,[5–7] as well as other Tl cuprates.[10,11,19,22,23] The Tl $4f_{7/2}$ binding energy, which in Tl cuprates is intermediate between Tl_2O and Tl_2O_3, has been interpreted[5–7,23] as evidence that Tl is in an intermediate oxidation state between 1+ and 3+, being nearly 3+ for Tl-1212. Similarly, the increase in the Tl $4f_{7/2}$ binding energy with decreased hole doping when Y^{3+} is substituted for Ca^{2+} has been interpreted[7] as a change in the Tl valence. However, in this work the primary effect of a change in the doping level is found to be a shift of the Fermi level, as discussed later.

The Ba $4d$ (Fig. 6) and $3d$ (not shown) spectra consist of the dominant superconductor signal and a lower-intensity contaminant signal at higher binding energy. An earlier study[6] of Tl-1212 found a Ba $3d_{5/2}$ binding energy 0.7 eV higher than that measured in this work. However, the O $1s$ signal exhibits a significantly higher contaminant signal in the earlier work[6] compared to this work, and the Ba $3d$ signal, with lower photoelectron kinetic energy, is more surface sensitive. Since the energy separation of the Ba $3d$ signals from the superconductor and contaminants is nearly the same as the peak width, the lower binding energy observed in this work reflects the lower level of contaminants. The band-structure results in Fig. 4 suggest that Ba atoms near O(3) vacancies should yield photoemission signals at ~ 2 eV lower binding energy than Ba atoms near occupied O(3) sites. Assuming 75% O(3) occupancy, the Ba signal should therefore consist of two signals with a 3:1 ratio between the high- and low-binding-energy components, which is not observed in Fig. 6. Some possible reasons for this apparent discrepancy are that the splitting of the states may be more pronounced for the shallow Ba $5p$ core levels, the band structure calculated for $\delta = 0.5$ may not be directly comparable to a doping level of $\delta = 0.25$, or the crystal structure determined for $\delta = 0.25$ may not be completely accurate for the calculations of the $\delta = 0, 0.5$ cases.

The Ca $2p$ spectrum in Fig. 7 consists of two doublets, as shown in the least-squares fitting results in Fig. 7, both of which are associated with Tl-1212. Prior to etching, a higher-binding-energy surface contaminant signal with a Ca $2p_{3/2}$ component near 347 eV is also prominent, but is not detectable after etching. The two doublets evident in Fig. 7 are also observed in the Ca $2p$ spectra of Hg-1212 (Ref. 9) and Tl-

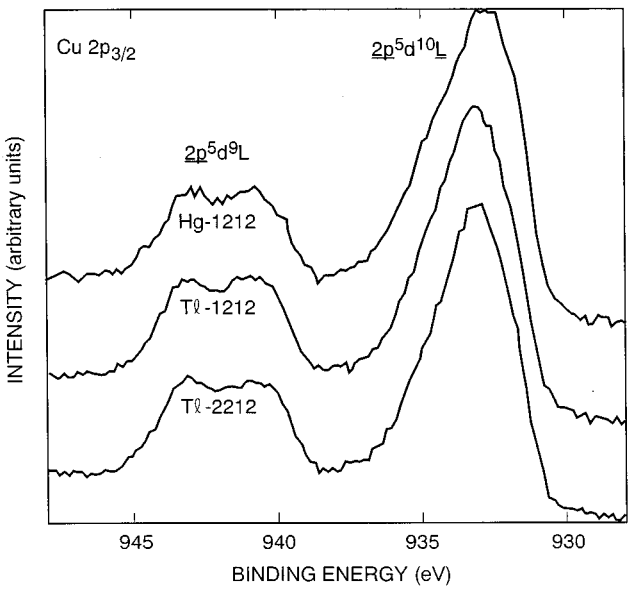

FIG. 8. Cu $2p_{3/2}$ spectra measured for Tl-1212 (this work), Tl-2212 (Ref. 10), and Hg-1212 (Ref. 9).

2212 (Ref. 10), as well as other Ca-containing cuprates such as $Bi_2Sr_2CaCu_2O_{8+\delta}$ (Bi-2212),[24] and have been interpreted as originating from occupation of inequivalent lattice sites due to cation disorder, with the lower-binding-energy doublet assigned to the site between Cu-O planes. As in other alkaline-earth compounds in general and cuprate superconductors in particular, the Ba and Ca core-level binding energies of Tl-1212 measured in this work are significantly lower than those of the corresponding metals, which has been attributed to initial-state electrostatic effects, specifically the Madelung energy being larger than the ionization energy.[24–27]

The Cu $2p_{3/2}$ spectra measured from Hg-1212, Tl-1212, and Tl-2212 are compared in Fig. 8, and are typical of Cu^{2+} compounds. The satellite at higher binding energy corresponds to a multiplet of $\underline{2p}^5 3d^9\underline{L}$ states, where underbar denotes a hole and $\underline{L}$ denotes the oxygen ligand, and the main peak near 933 eV is usually attributed to well-screened $\underline{2p}^5 3d^{10}\underline{L}$ final states resulting from ligand-to-metal (O $\underline{2p} \rightarrow$ Cu $\underline{3d}$) charge transfer.[28–30] The relatively large width (>3 eV) and asymmetry of the 933 eV signal cannot be explained by core-hole lifetime broadening or instrumental resolution, or by multiplet splitting, which would not be expected when the Cu $3d$ states are fully occupied, and are usually attributed to O $2p$ band effects. The main peak binding energy and width and the satellite/main intensity ratio I_s/I_m for Tl-1212 measured in this work are in general agreement with those reported for Tl-1212 polycrystalline pellets scraped in vacuum.[6,7] The satellite–main-peak energy separation and I_s/I_m are related to the O $2p$–Cu $3d$ hybridization and charge-transfer energy,[29,30] the similarity of the Cu $2p_{3/2}$ spectra for Tl-1212 and Tl-2212 (see Fig. 8 and Table I) thus indicates that the number of Tl-O layers has little effect on the Cu-O bonding. However, the Tl-1212 and Hg-1212 Cu $2p_{3/2}$ signals do differ, with the Hg-1212 signal having a lower value of I_s/I_m and the main signal being broader on the low-binding-energy side. Such observations could be an indication of oxygen deficiency in Hg-1212, which would be accompanied by an increased intensity on the high-binding-energy side of the O $1s$ signal (near 529 eV; e.g., see Refs. 21 and 31). This possibility can be eliminated by examination of Fig. 5, which shows that the Hg-1212 O $1s$ signal has enhanced intensity at lower binding energy compared to the Tl-1212 signal. The observed differences in the Tl-1212 and Hg-1212 Cu $2p_{3/2}$ signals thus appear to be intrinsic. The lower value of I_s/I_m observed for Hg-1212 indicates that replacement of Tl^{3+} with Hg^{2+} results in a lowering of the O $2p \rightarrow$ Cu $3d$ charge-transfer energy. The observed differences in the Cu $2p_{3/2}$ main peak widths, according to the conventional interpretation, should reflect differences in the O $2p$ bandwidths. The calculated O $2p$ bandwidth for Hg-1212 (Ref. 32) does not differ significantly from that for Tl-1212 (see Fig. 1), though if electron correlation effects differ significantly in the two materials, then O $2p$ bandwidth differences could result due to the Cu $3d$–O $2p$ hybridization. Other possibilities are considered below.

Two models have recently been proposed which result in the Cu $2p_{3/2}$ main peak having contributions from more than one final state. In one model, the Cu $2p_{3/2}$ main peak consists of two final states corresponding to charge transfer from Cu-O plane oxygens (O $2p_{x,y} \rightarrow$ Cu $3d_{x^2-y^2}$) and apical oxygens (O $2p_z \rightarrow$ Cu $3d_{z^2}$).[33] This model is consistent with the larger Cu $2p_{3/2}$ main peak widths and asymmetric line shapes (skewed towards higher binding energy) observed from Cu compounds with pyramidal or octahedral oxygen coordination compared to compounds with square planar oxygen coordination. However, Tl-1212 and Hg-1212 are isostructural, with Cu having pyramidal oxygen coordination in both compounds. If this model is correct, then the observed line shape differences may reflect differences in the planar vs apical oxygen charge-transfer probabilities. In the second model, the Cu $2p_{3/2}$ main peak consists of $\underline{2p}^5 3d^{10}\underline{L}$ final states at higher binding energy and lower-binding-energy $\underline{2p}^5 3d^{10}$ final states which result from core-hole repulsion yielding Zhang-Rice singlet states.[34] If this model is correct, then the observed line shape differences may reflect differences in the probability of Zhang-Rice singlet-state formation. Both mechanisms may contribute to the Cu $2p_{3/2}$ main peak width and complex line shape.

V. EFFECT OF DOPING ON THE CHEMICAL POTENTIAL

Tl-1212 is unusual in that even for a stoichiometric oxygen content ($\delta=0$), the Fermi level lies below the VHS seen so prominently in Fig. 3 at the R point (E_F typically lies above the VHS and hole doping is required to lower it onto the VHS). In several models,[35] the VHS is regarded as one of the main reasons for high-T_c superconductivity. However, the recent observations of an extended VHS near the Fermi level for Bi-2201 ($T_c \sim 10$ K) (Ref. 36) and Sr_2RuO_4 ($T_c \sim 1$ K) (Refs. 37 and 38) suggest that the VHS may be necessary but not sufficient for producing high-T_c superconductivity. Even though the VHS may not be directly responsible for high-T_c superconductivity, the role of the VHS in those compounds which do exhibit high-T_c superconductiv-

ity appears to be that an optimum T_c is associated with an E_F shifted onto or close to the VHS. Thus the fact that E_F crosses the X-R line of the VHS makes it understandable why samples of Tl-1212 synthesized in oxygen are already high-T_c superconductors. In order to increase T_c further, E_F must shift upwards onto the prominent VHS at the R point.

The core levels measured in this work from both nitrogen-annealed Tl-1212 films are consistently observed at slightly higher binding energies than those of the as-grown sample (see Table I). With the exception of the Cu $2p_{3/2}$ signal, for which the width of the signal makes detection of small shifts difficult, these binding-energy shifts (± 0.05 eV) are in the range 0.04–0.11 eV for the $T_c = 87$ K sample and 0.04–0.17 eV for the $T_c = 86$ K sample. The higher values may be more reliable, since the lower values are from the Ca $2p$ and O $1s$ signals, which consist of overlapping components whose binding energies determined from least-squares fitting may have greater uncertainty. Core potential differences due to changes in effective charges or to changes in the Madelung potential (e.g., from bond length changes) would be expected to have opposite effects on different sites. The observed shifts in the core-level binding energies in the same direction by nearly the same amount (within experimental error) with doping thus suggest that the change in the chemical potential is the dominant effect of doping. Doping-induced changes in chemical potentials have previously been reported for Tl-2201,[11] as well as for other cuprates.[39–43]

During the process of annealing in nitrogen, oxygen is depleted from the O(3) position (since, as indicated above, it is the weakest bonded ion) and so adds electrons to the conduction band. As shown by the Tl-1212 ($\delta = 0.5$) calculations, this shifts E_F onto the VHS at the R point. The observations that T_c increases and the core levels shift to higher binding energies with nitrogen annealing are consistent with a reduction in the level of hole doping and a shift of E_F close to the VHS that are expected with the removal of oxygen. Clearly, in this view, the same effect could also be achieved through trivalent ion substitutions for Ca. In fact, substitution of Nd, Gd, or Y for Ca in Tl-1212 has been reported to increase T_c, with maximum T_c occurring for 30% substitution,[44] and substitution of Y for Ca has been reported to result in an increased Tl $4f_{7/2}$ binding energy.[7] In the latter study, the increased Tl $4f_{7/2}$ binding energy was interpreted as evidence for a change in the Tl valence, rather than a change in the chemical potential, since the Cu $2p_{3/2}$ binding energy was not doping dependent. It is difficult to assess the validity of this interpretation since other core-level measurements were not reported. However, the possibility that a Fermi-level shift could have been masked is suggested by the higher levels of surface contaminants in the earlier studies[5–7] and the greater surface sensitivity and large width of the Cu $2p_{3/2}$ signal.

VI. XPS VALENCE-BAND MEASUREMENTS

Figure 9 compares the valence bands and the Tl $5d$ and Ba $5p$ shallow core levels of Tl-1212 and Tl-2212, scaled to facilitate comparison of the line shape differences in the valence-band region. The Fermi edges, not reported in earlier studies of Tl-1212,[5–7] are shown more clearly in the inset,

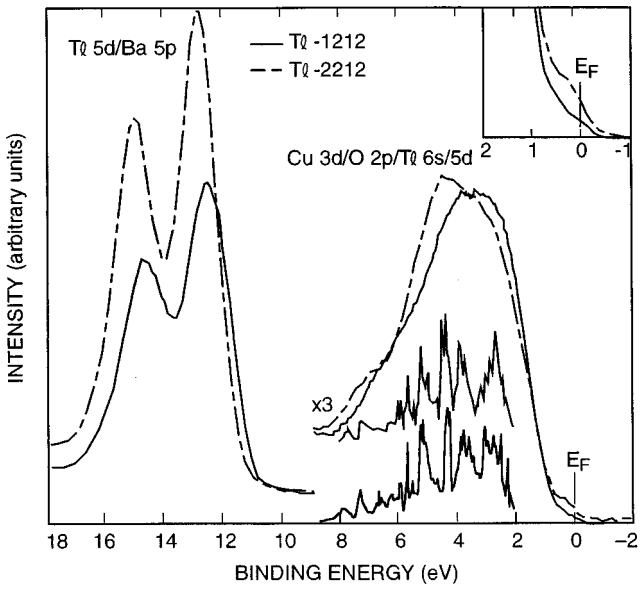

FIG. 9. Valence bands and Tl $5d$/Ba $5p$ shallow core-level spectra measured from Tl-1212 (this work) and Tl-2212 (Ref. 10), scaled to facilitate comparison of the valence-band features. The inset shows the Fermi edges. Below the valence bands are the calculated Cu $3d$ partial densities of states of Tl-1212 (top, this work) and Tl-2212 (bottom, from Ref. 47).

further demonstrating the surface quality. The valence bands consist primarily of Cu $3d$, O $2p$, and Tl $6s/5d$ states, with the Cu and Tl states contributing most of the spectral weight for the photon energy used in this work.[45,46] Distinct differences in the measured Tl-1212 and Tl-2212 DOS are apparent in Fig. 9. The shoulder near 7 eV in the Tl-2212 spectrum consists primarily of Tl $6s$ states.[46,47] This feature is relatively less prominent in the Tl-1212 spectrum, reflecting both the smaller Tl/Cu ratio relative to Tl-2212 and the occurrence of the Tl $6s$ states at lower binding energy, near 5 eV (see Fig. 1). Tl-2212 also exhibits significant Tl $6s/5d$ spectral weight throughout the energy range 3–7 eV,[46] so that the larger Tl/Cu ratio relative to Tl-1212 is consistent with the larger observed relative intensity at greater than 4 eV binding energy. However, the Tl-1212 valence-band shape is more skewed towards high binding energy despite the lower Tl partial DOS in this region. Below the valence bands in Fig. 9 are the Cu $3d$ partial DOS (the primary contributions to the measured valence bands) from band-structure calculations of Tl-1212 (top, this work) and Tl-2212 (bottom, Ref. 47), shifted by 2 eV to approximately match the envelopes of the valence bands. Electron correlation effects have often been cited as necessitating similar shifts for other cuprate superconductors. The skewing of the Tl-1212 valence band towards higher binding energy may be a reflection of the more sharply peaked Cu $3d$ partial DOS in the region 5–6 eV.

The valence bands and shallow core levels of Tl-1212 and Hg-1212 are compared in Fig. 10. The most striking difference in the valence bands is the increased intensity near 5 eV in the Hg-1212 spectrum. The Hg-1212 Cu $3d$ partial DOS is similar to that of Tl-2212 (see the comparison in Ref. 9), and the differences with Tl-1212 are not sufficient to account for the observed spectra. Shown below the valence bands in

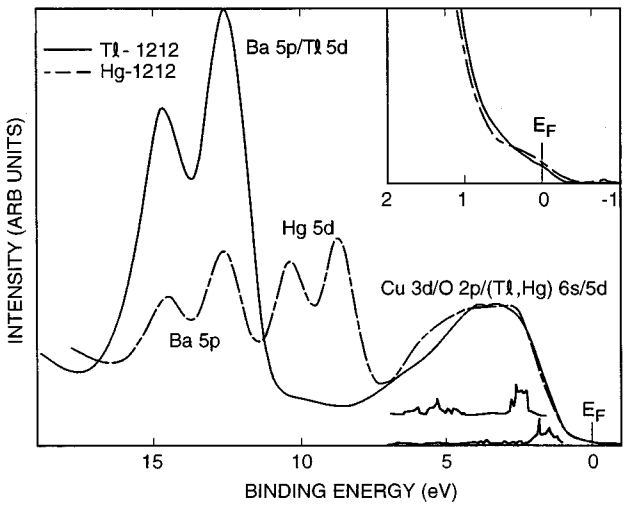

FIG. 10. Valence bands and shallow core levels measured for Tl-1212 (this work) and Hg-1212 (Ref. 9), scaled to facilitate comparison of the valence-band features. The inset shows the Fermi edges. Below the valence bands are the calculated Tl-1212 Tl 5*d* (bottom, this work) and Hg-1212 Hg 5*d* (bottom, from Ref. 32) partial densities of states in the binding-energy range 2–7 eV.

Fig. 10 are the Hg-1212 Hg 5*d* (top, Ref. 32) and Tl-1212 Tl 5*d* (bottom, this work) partial DOS in the energy range of interest. The occurrence of Hg 5*d* states near 5 eV for Hg-1212 and the lack of corresponding states for Tl-1212 are consistent with the observed differences in the measured valence bands.

Within the accuracy of the experimental measurements, no significant differences are observed in the valence bands of Tl-1212 samples with different oxygen doping levels. Comparing Figs. 1 and 4, doping affects primarily the O (2,3) 2*p* states in the valence-band region. However, for the photon energy used in this work, the photoionization cross section of O 2*p* states is two orders of magnitude smaller than that of Cu 3*d* states,[45] making changes in the O 2*p* states undetectable in this work. The primary detectable effect of doping differences is the core-level shifts resulting from the change in chemical potential, as previously discussed.

VII. SUMMARY AND CONCLUSIONS

The core levels of high-quality Tl-1212 epitaxial films were measured with XPS, and the valence electronic structure was determined by band-structure calculations and measured with XPS. The surface quality has been demonstrated by the low level of high-binding-energy signals from contaminants in the O 1*s* and alkaline-earth core-level regions and by the observation of a Fermi edge in the valence-band region. The O 1*s* signal is resolved into two components, associated with Cu-O planes and Tl-O bonding. The similarity of the Tl-1212 and Tl-2212 Cu $2p_{3/2}$ spectra shows that the number of Tl-O layers has little effect on the Cu-O bonding. However, the Tl-1212 and Hg-1212 Cu $2p_{3/2}$ signals exhibit differences which suggest that the replacement of Tl^{3+} with Hg^{2+} results in a decrease in the O $2p \rightarrow$Cu $3d$ charge-transfer energy, as well as differences in the probabilities of planar vs apical oxygen charge transfer and/or Zhang-Rice singlet-state formation. Measurements from samples with differing T_c's resulting from differing oxygen doping levels show that, within experimental error, the core levels are rigidly shifted, consistent with a doping-induced change in chemical potential. The band-structure calculations show that for the stoichiometric compound ($\delta=0$) the van Hove singularity is above E_F and is close to E_F for $\delta=0.5$. Samples annealed in nitrogen (to reduce the hole overdoping by the removal of oxygen) exhibit higher core-level binding energies and higher T_c, consistent with a shift of E_F onto or nearer the VHS. Differences between the valence bands of Tl-1212 measured in this work and previously measured Tl-2212 and Hg-1212 valence bands are consistent with differences in the calculated Cu 3*d* and (Tl, Hg) 6*s*/5*d* partial DOS.

ACKNOWLEDGMENTS

Part of the work described in this paper was performed by the Center for Space Microelectronics Technology, Jet Propulsion Laboratory, California Institute of Technology, and was sponsored by the National Aeronautics and Space Administration, Office of Space Science. The work at Northwestern University was supported by the National Science Foundation (DMR 91-20000) through the Northwestern University Science and Technology Center for Superconductivity and a grant of supercomputing time at the NSF-supported Pittsburgh Supercomputing Center. Part of this work was performed at Sandia National Laboratories, Albuquerque, NM, and supported by the U.S. Department of Energy, Office of Basic Energy Sciences under Contract No. DE-ACO4-94AL85000.

[1] S. V. Meshkov, S. N. Molotkov, S. S. Nazin, I. S. Smirnova, and V. V. Tatarskii, Physica C **166**, 476 (1990).

[2] S. Nakajima, M. Kikuchi, Y. Syono, K. Nagase, T. Oku, N. Kobayashi, D. Shindo, and K. Hiraga, Physica C **170**, 443 (1990).

[3] M. P. Siegal, N. Missert, E. L. Venturini, P. P. Newcomer, F. Dominguez, and R. Dunn, IEEE Trans. Appl. Supercond. **AS-5**, 1343 (1995).

[4] M. P. Siegal, E. L. Venturini, P. P. Newcomer, B. Morosin, D. L. Overmyer, F. Dominguez, and R. Dunn, Appl. Phys. Lett. **67**, 3966 (1995).

[5] T. Suzuki, M. Nagoshi, Y. Fukuda, S. Nakajima, M. Kikuchi, Y. Syono, and M. Tachiki, Physica C **162-164**, 1387 (1989).

[6] Y. Fukuda, T. Suzuki, and M. Nagoshi, in *Thallium-Based High Temperature Superconductors*, edited by A. M. Hermann and J. V. Yakhmi (Dekker, New York, 1994), Chap. 24, pp. 511–522.

[7] T. Suzuki, M. Nagoshi, Y. Fukuda, S. Nakajima, M. Kikuchi, Y. Syono, and M. Tachiki, Supercond. Sci. Technol. **7**, 817 (1994).

[8] R. P. Vasquez, J. Electron Spectrosc. Relat. Phenom. **66**, 209 (1994), and references therein.
[9] R. P. Vasquez, M. Rupp, A. Gupta, and C. C. Tsuei, Phys. Rev. B **51**, 15 657 (1995).
[10] R. P. Vasquez and W. L. Olson, Physica C **177**, 223 (1991).
[11] R. P. Vasquez, Z. F. Ren, and J. H. Wang, Phys. Rev. B **54**, 6115 (1996).
[12] M. Methfessel, Phys. Rev. B **38**, 1537 (1988).
[13] B. Morosin, D. S. Ginley, P. F. Hlava, M. J. Carr, R. J. Baughman, J. E. Schirber, E. L. Venturini, and J. F. Kwak, Physica C **152**, 413 (1988).
[14] M. Schilfgaarde (unpublished).
[15] D. Singh, *Planewaves, Pseudopotentials and the LAPW Method* (Kluwer Academic, Dordrecht, The Netherlands, 1994); Phys. Rev. B **43**, 6388 (1991).
[16] D. L. Novikov and A. J. Freeman, in *Recent Developments in High Temperature Superconductivity*, edited by J. Klamut, B. W. Veal, B. M. Dabrowski, P. W. Klamut, and M. Kazimierski, Lecture Notes in Physics, Vol. 475 (Springer-Verlag, New York, 1996).
[17] J. H. Weaver, H. M. Meyer III, T. J. Wagener, D. M. Hill, Y. Gao, D. Peterson, Z. Fisk, and A. J. Arko, Phys. Rev. B **38**, 4668 (1988).
[18] H. M. Mayer III, D. M. Hill, J. H. Weaver, D. L. Nelson, and C. F. Gallo, Phys. Rev. B **38**, 7144 (1988).
[19] H. M. Meyer III, T. J. Wagener, J. H. Weaver, and D. S. Ginley, Phys. Rev. B **39**, 7343 (1989).
[20] F. Parmigiani, Z. X. Shen, D. B. Mitzi, I. Lindau, W. E. Spicer, and A. Kapitulnick, Phys. Rev. B **43**, 3085 (1991).
[21] R. P. Vasquez, B. D. Hunt, M. C. Foote, L. J. Bajuk, and W. L. Olson, Physica C **190**, 249 (1992).
[22] A. E. Bocquet, J. F. Dobson, P. C. Healey, S. Myrha, and J. G. Thompson, Phys. Status Solidi B **152**, 519 (1989).
[23] T. Suzuki, M. Nagoshi, Y. Fukuda, Y. Syono, M. Kikuchi, N. Kobayashi, and M. Tachiki, Phys. Rev. B **40**, 5184 (1989).
[24] R. P. Vasquez, J. Electron Spectrosc. Relat. Phenom. **66**, 241 (1994), and references therein.
[25] R. P. Vasquez, J. Electron Spectrosc. Relat. Phenom. **56**, 217 (1991).
[26] C. Sousa, T. Minerva, G. Pacchioni, P. S. Bagus, and F. Parmigiani, J. Electron. Spectrosc. Relat. Phenom. **63**, 189 (1993).
[27] M. Nagoshi, Y. Syono, M. Tachiki, and Y. Fukuda, Phys. Rev. B **51**, 9352 (1995).
[28] S. Larsson, Chem. Phys. Lett. **40**, 362 (1976).
[29] G. van der Laan, C. Westra, C. Haas, and G. A. Sawatzky, Phys. Rev. B **23**, 4369 (1981).
[30] F. Parmigiani and L. Sangaletti, J. Electron Spectrosc. Relat. Phenom. **66**, 223 (1994), and references therein.
[31] R. P. Vasquez, M. C. Foote, L. Bajuk, and B. D. Hunt, J. Electron Spectrosc. Relat. Phenom. **57**, 317 (1991).
[32] D. L. Novikov and A. J. Freeman, Physica C **216**, 273 (1993).
[33] F. Parmigiani, L. E. Depero, T. Minerva, and J. B. Torrance, J. Electron Spectrosc. Relat. Phenom. **58**, 315 (1992).
[34] M. A. van Veenendaal, H. Eskes, and G. A. Sawatzky, Phys. Rev. B **47**, 11 462 (1993).
[35] R. S. Markiewicz, Physica C **217**, 381 (1993).
[36] D. M. King, Z.-X. Shen, D. S. Dessau, D. S. Marshall, C. H. Park, W. E. Spicer, J. L. Peng, Z. Y. Li, and R. L. Greene, Phys. Rev. Lett. **73**, 3298 (1994).
[37] T. Yokoya, A. Chainani, T. Takahashi, H. Katayama-Yoshida, M. Kasai, and Y. Tokura, Phys. Rev. Lett. **76**, 3009 (1996).
[38] D. H. Lu, M. Schmidt, T. R. Cummins, S. Schuppler, F. Lichtenberg, and J. G. Bednorz, Phys. Rev. Lett. **76**, 4845 (1996).
[39] Z.-X. Shen, D. S. Dessau, B. O. Wells, C. G. Olson, D. B. Mitzi, L. Lombardo, R. S. List, and R. J. Arko, Phys. Rev. B **44**, 12 098 (1991).
[40] M. A. van Veenendaal, R. Schlatmann, G. A. Sawatzky, and W. A. Groen, Phys. Rev. B **47**, 446 (1993).
[41] M. A. van Veenendaal, G. A. Sawatzky, and W. A. Groen, Phys. Rev. B **49**, 1407 (1994).
[42] G. Rietveld, M. Glastra, and D. van der Marel, Physica C **241**, 257 (1995).
[43] G. Rietveld, S. J. Collocott, R. Driver, and D. van der Marel, Physica C **241**, 273 (1995).
[44] S. Nakajima, M. Kikuchi, Y. Syono, N. Kobayashi, and Y. Muto, Physica C **168**, 57 (1989).
[45] J. J. Yeh and I. Lindau, At. Data Nucl. Data Tables **32**, 1 (1985).
[46] P. Marksteiner, J. Yu, S. Massidda, A. J. Freeman, J. Redinger, and P. Weinberger, Phys. Rev. B **39**, 2894 (1989).
[47] J. Yu, S. Massidda, and A. J. Freeman, Physica C **152**, 273 (1988).